Front. Mater. Sci. 2024, 18(2): 240682
https://doi.org/10.1007/s11706-024-0682-z

RESEARCH ARTICLE

Hydrogel-supported poly(L-lactic acid) and polystyrene microsphere-based three-dimensional culture systems for *in vitro* cell expansion

Huaying Hao[2], Lihong Sun[3], Jiaxuan Chen[2], and Jun Liang (✉)[1,2]

1 State Key Laboratory of Food Nutrition and Safety, Tianjin University of Science & Technology, Tianjin 300457, China
2 College of Light Industry Science and Engineering, Tianjin University of Science & Technology, Tianjin 300457, China
3 College of Food Science and Engineering, Tianjin University of Science & Technology, Tianjin 300457, China

ABSTRACT: The *in vitro* expansion of stem cells is important for their application in different life science fields such as cellular tissue and organ repair. An objective of this paper was to achieve static cell culture *in vitro* through peptide hydrogel-supported microspheres (MSs). The peptides, with their gel-forming properties, microstructures, and mechanical strengths characterized, were found to have good support for the MSs and to be injectable. The internal structures of poly(L-lactic acid) microspheres (PLLA-MSs) and polystyrene microspheres (PS-MSs) made in the laboratory were observed and statistically analyzed in terms of particle size and pore size, following which the co-cultured MSs with cells were found to have good cell adhesion. In addition, three-dimensional (3D) culturing of cells was performed on the peptide and microcarrier composite scaffolds to measure cell viability and cell proliferation. The results showed that the peptides could be stimulated by the culture medium to self-assembly form a 3D fiber network structure. Under the peptide-MS composite scaffold-based cell culture system, further enhancement of the cell culture effect was measured. The peptide-MS composite scaffolds have great potential for the application in 3D cell culture and *in vitro* cell expansion.

KEYWORDS: microcarrier; microsphere; peptide hydrogel; cell scaffold; three-dimensional culture; cell expansion

Contents

Received October 27, 2023; accepted March 10, 2024

E-mail: jliang1118@yeah.net

1 Introduction

For tissue engineering applications, hydrogel, a three-dimensional (3D) crosslinked macromolecular network primarily made of water, is the perfect kind of biomaterial [1–3]. Both synthetic polymers and biological macromolecules have been effectively constructed in recent years for the production of hydrogel scaffolds [4–5]. Because of their superior biocompatibility and bioactivities, natural macromolecules like collagen and Matrigel [6–10] have been employed as scaffolds. However, due to the limitations such as batch-to-batch variations, inclusion of undesirable residues, and challenges to preservation of functionality after chemical modifications, the use of natural macromolecules has been restricted [11]. The easy modification of synthetic hydrogels, on the other hand, leads to the development of hydrogel systems with better physicochemical characteristics for tissue engineering applications [12]. This is because altering the polymer structure or the amount of intermolecular crosslinking allows for the simplicity in the tuning of hydrogel properties [2,13–15]. Despite this, employing synthetic polymers as 3D scaffolds has several disadvantages, e.g., the absence of biological functions, the possibility of inflammatory responses, and the cytotoxicity brought on by chemical crosslinking [16–18]. The biomedical community has paid close attention to synthetic peptides that combine the advantages of both synthetic polymers and natural macromolecules, including ease of modulation, consistency, high biocompatibility, and bioactivity [19–20]. The advancement of peptides in tissue engineering is further promoted by the identification of those having self-assembling capabilities [20].

Owing to its high surface area-to-volume ratio for the large-scale growth of anchorage-dependent cells such as mesenchymal stem cells (MSCs) [21–22] and embryonic stem cells (ESCs), the microsphere (MS)-based cell culture system is regarded to have superiority in the expansion of cells. Given that it offers more surface area for growth of cells and demands less space and culture medium than those of traditional two-dimensional (2D) culture systems, the MS-based cell culture system demonstrates potential in solving the difficulty of growing cells in enough quantity to meet clinical requirements. Moreover, cell culture conditions such as oxygen content, pH, and nutrient transport process are also controllable when the MS-based cell expansion method is used in conjunction with bioreactors [23].

Natural and synthetic polymers as well as decellularized tissues have been frequently utilized for the manufacturing of MSs because they can facilitate the necessary assurance of materials' quality on aspects of biocompatibility, biodegradability, bioactivity, etc. Contrary to their natural equivalents, synthetic polymers such as poly(lactic-co-glycolic acid) (PLGA) [24–25], polystyrene (PS) [26], and poly(L-lactic acid) (PLLA) [27] are easily scaled up for use in the bulk expansion of cells. Due to their endowed biocompatibility, non-toxicity, and ease of modification, biodegradable synthetic polymers such as PLLA are regarded among the best materials for the fabrication of biodegradable MSs [28–30], and one of synthetic polymers most commercially utilized is PS [31].

In this study, two types of MSs were selected for culturing cells, with their morphologies, particle sizes, and pore sizes analyzed through optical microscopy (OM), transmission electron microscopy (TEM), and scanning electron microscopy (SEM). Additionally, bone marrow mesenchymal stem cells (BMSCs) inoculated on MSs were cultured *in vitro*, aiming to investigate the effects of selected materials on the proliferation of stem cells either in the static mode with the addition of peptide scaffolds (but not in a biological reactor) or in the mode with the immobilization in culturing media. We believe that under the culturing mode with peptide-MS composite scaffolds, stem cells can effectively expand *in vitro*, presenting potential applications of such scaffolds in the field of tissue engineering.

2 Experimental

2.1 Preparation of MSs

PLLA-MSs were prepared via the modified emulsion-solvent evaporation method [32–34]. The received

PLLA-MSs were then separated using standard testing sieves and those with a diameter of 150–400 μm were collected for further hydrolysis modification [35]. PS-MSs were prepared by the droplet polymerization method. Dibenzoyl peroxide was first dissolved with styrene and divinylbenzene, and then n-heptane was added, followed by uniform mixing. After the poly(vinyl alcohol) (PVA) solution (100 mL, 2.5 wt.%) was further mixed with above chemicals, they reacted in a beaker. The oxygen was subsequently removed by bubbling N_2 throughout the process. The reaction temperature and stirring rate were set to 70 °C and 220 $r \cdot min^{-1}$, respectively, while the reaction time was 12 h. After the heating was stopped, the mixer remained rotating until the temperature dropped to below 50 °C. Finally the PS-MSs were poured out, followed by filtration through a sieve.

2.2 Preparation of hydrogels

Commercial hydrogels (CulX I) were prepared following the protocols provided by CytoPort LLC (Tianjin, China). CulX I freeze-dried power was mixed with a commonly used culture medium, α-modified Eagle's medium (α-MEM), for culturing BMSCs at desirable concentrations. The mixture was then incubated at room temperature for 30 min to form hydrogels.

2.3 TEM measurements

TEM was performed on preincubated peptide or peptide-triggered hybrid samples (0.3 wt.%). A droplet of each suspension (10 μL) was deposited on a Formvar/carbon-coated 300-mesh copper grid, following which it was dried in air. The samples were then stained with 2% phosphotungstic acid (PWA) solution followed by incubation for 60 s. After that, excess water on grids was removed with filter paper. Such a staining process was repeated three times. Afterwards, the samples were dried again. Finally, TEM images were acquired with a transmission electron microscope (Talos F200X G2, USA).

2.4 SEM measurements

The nanofiber network of peptide scaffolds and peptide-triggered hybrid samples with the concentration of 1.0 wt.% was observed through SEM. A droplet of each sample (10 μL) was deposited on a silicon wafer, followed by drying in air. Then the sample was covered with gold by a sputter-coater (Cressington 108, Lycra, Germany). SEM images were finally obtained on a scanning electron microscope (JSM-IT300LV, Japan) operated at an acceleration voltage of 10 kV.

2.5 Rheological tests

Mechanical properties of peptide hydrogels were measured on a rheometer (HAAKE Mars60, Thermo Fisher, Germany) with a parallel-plate geometry 20 mm in diameter at 37 °C. Hydrogels with various concentrations of 0.3, 0.5, and 1.0 wt.% were first prepared according to the above protocol. Such hydrogels (200 μL) were then pipetted onto the plate and the geometry was lowered to a gap distance of 0.5 mm. Afterwards, time sweep measurements were conducted at a frequency of 1.0 Hz with a strain of 1%, while frequency sweep tests were conducted from 0.1 to 10 Hz at 1% strain. Subsequently, a step-strain measurement was performed after the plateau in the storage modulus was reached in the time sweep process. After 100% strain was applied for 30 s, those peptide hydrogels were left to recover for 15 min while measuring at 1% strain (f = 1.0 Hz), during which the storage modulus returned to the original plateau. Such a measurement was repeated for three cycles.

2.6 Cell culture

BMSCs were cultured in Dulbecco's modified Eagle's medium (DMEM) with 10% fetal bovine serum (FBS) and 1% penicillin–streptomycin contained by an incubator at 37 °C with 5% CO_2. Once reaching confluence, cells were trypsinized and resuspended in the culture medium at a certain density for further use. Before cell experiments, PS-MSs and PLLA-MSs 100–300 μm in size were obtained by filtration through a cell sieve followed by sterilization. Sterilized MSs were then immersed in the cell culture medium, and 20 μL of the resulted MS suspension was added into each well of 96-well plates, following which BMSCs at the concentration of 2×10^4 cells/well were seeded onto those MSs and cultured for 24 h to ensure cell attachment on the MS surface. After the hydrogel at a concentration of 0.3 wt.% was added, hydrogel–MS–cells were finally mixed through gentle blowing, followed by incubation in a humidified incubator containing 5% CO_2 with the temperature maintained at 37 °C.

2.7 Cell morphology

SEM was carried out to characterize the cell adhesion on both types of MSs. After culturing for 1 d, BMSCs-loaded microcarriers were immediately rinsed with phosphate buffer saline (PBS) and soaked in a glutaraldehyde solution at 4 °C for 20 min. Afterwards, the fixed samples were dehydrated through a graded series of ethanol solutions with increased concentrations (i.e., 70%, 80%, 90%, and 100%), followed by drying under vacuum. The samples were then sputter-coated with platinum for SEM observation.

2.8 Cell viability assay

A live/dead staining assay was used to evaluate the viability of cells. Briefly, calcein acetoxymethyl ester (calcein-AM) and propidium iodide (PI) were mixed at a ratio of 1:1.5 with 1 mL PBS. After the medium was discarded, the cultured samples were washed twice with PBS, following which the BMSCs-loaded microcarriers were stained for 15 min at room temperature. Subsequently, the samples were washed again with PBS, followed by visualization through confocal laser scanning microscopy (CLSM), in which dead cells exhibited the red fluorescence, while live cells showed the green one.

2.9 Characterization of cell proliferation

BMSCs were seeded onto both types of MSs, and their cell proliferations were evaluated using Cell Counting Kit-8 (CCK-8) assay (Solarbio Co., Ltd., Beijing, China). First, 2×10^4 cells were seeded onto both types of sterilized MSs in a 96-well plate, each with 0.1 mL culture medium. After cell seeding and subsequent culturing for 1, 4, and 7 d, the liquid in each well was discarded, followed by the addition of CCK-8 solution (10% in α-MEM) and the incubation at 37 °C with 5% CO_2 for 1 h. The supernatant was finally collected, with its absorbance measured at 450 nm using a microplate reader (Bio-Rad, Shanghai, China).

3 Results and discussion

3.1 Morphological and physical properties of MSs

Morphologies of both PLLA-MSs and PS-MSs were observed by OM and SEM at an accelerating voltage of 10 kV. The mean diameter of MSs was calculated through measuring about 100 MSs in multiple OM images, while the mean pore size of MSs was measured based on multiple SEM images using ImageJ software. Figure 1 shows morphologies of different types of MSs (PLLA and PS), from which it is seen that those MSs have good dispersibility and stability with porous structures. The average particle size of PLLA-MSs is about 210.2 μm revealed by Fig. 1(c), while about 145.48 μm for PS-MSs revealed by Fig. 1(d). PLLA-MSs can form a fine porous structure from the inside to the outside, resulting in a high

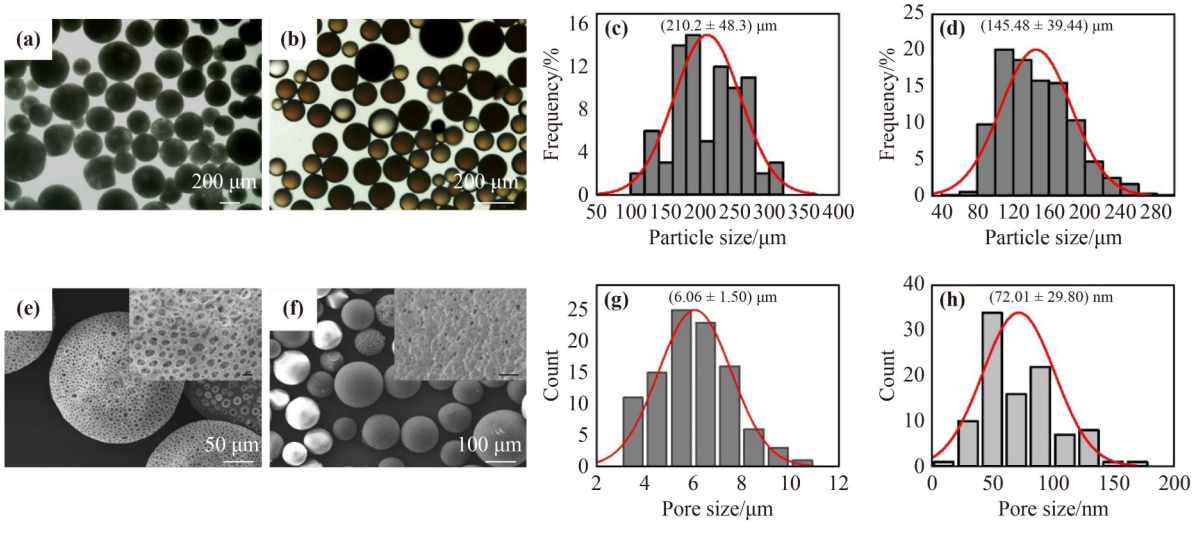

Fig. 1 Morphologies of MSs: outline drawings of (**a**) PLLA-MS and (**b**) PS-MS; size distributions of (**c**) PLLA-MS and (**d**) PS-MS; surface morphologies of (**e**) PLLA-MS and (**f**) PS-MS; pore size distributions of (**g**) PLLA-MS and (h) PS-MS.

porosity with the pore size of about 6 μm shown in Fig. 1(g). It is indeed suggested that large pore size and high pore interconnectivity within engineered scaffolds promote the diffusion of oxygen and nutrients, facilitating the growth and distribution of cells throughout the constructs [36–37]. The introduction of a porous structure with the pore size of approximately 72 nm in PS-MSs leads to an increase in the specific surface area (SSA) of MSs, which is able to provide more sites for the growth of cells.

3.2 Microstructural characterization of peptides

TEM and SEM were performed to investigate the microstructure of peptides. In the peptide solution, short and thin fibers with an erratic distribution are observed from the TEM image in Fig. 2(a). In contrast, in the presence of triggers, the integration of short fibers occurred in the peptide solution, resulting in the formation of a porous and highly organized scattered structure as shown in Fig. 2(b). It is also seen that peptides and triggers merge to form a highly porous structure according to the SEM image in Fig. 2(d), similar to the result from TEM. The resulted dense nanofibrous network can help enclosing cells in the 3D structure, effectively maintaining the moisture.

3.3 Mechanical properties of peptide scaffold materials

Rheological tests were carried out to research the mechanical characteristics of peptide self-assembly. From Fig. 3(a), it is seen that the peptide responded to self-assembly intelligently under the influence of the trigger, and the storage modulus (G') exhibited a gradient-dependent effect. It is also discovered that the G' value

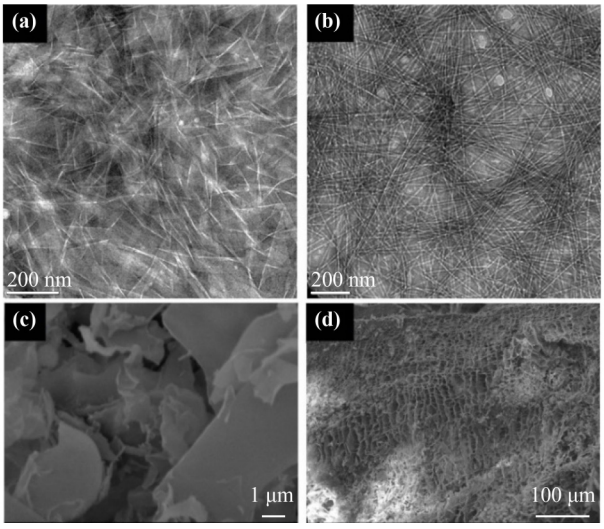

Fig. 2 Characterization of peptides: TEM images of (**a**) peptides (0.3 wt.%) and (**b**) peptides binding with the trigger (0.3 wt.%); SEM images of (**c**) peptides (1.0 wt.%) and (**d**) peptides binding with the trigger (1.0 wt.%).

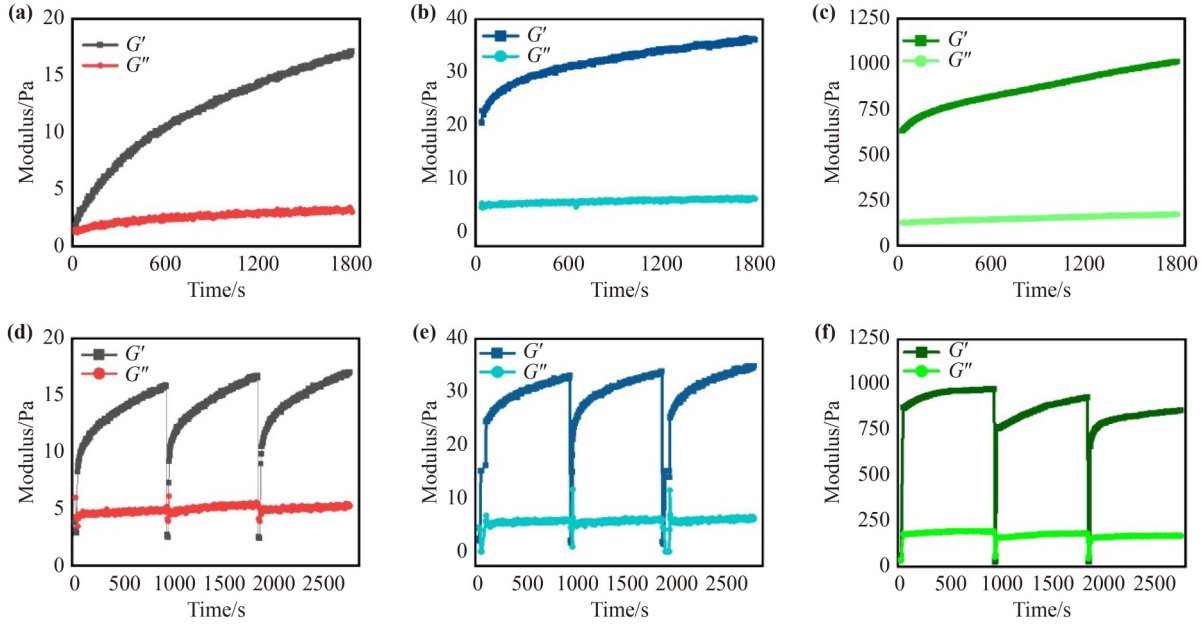

Fig. 3 Mechanical properties of peptides: time dependencies of storage modulus (G') and loss modulus (G'') values for peptide hydrogels with different concentrations of (**a**) 0.3 wt.%, (**b**) 0.5 wt.%, and (**c**) 1.0 wt.%; shear-thinning and recovery processes for peptides with different concentrations of (**d**) 0.3 wt.%, (**e**) 0.5 wt.%, and (**f**) 1.0 wt.% during the dynamic time sweep test.

increased with the enhancement of the peptide concentration. At the concentrations of 0.3, 0.5, and 1.0 wt.%, the peptide self-assembly led to stable G' values of roughly 17, 36, and 1012 Pa depicted in Figs. 3(a)–3(c), respectively. When the external strain was 100%, the peptide hydrogel exhibited a shear-thinning behavior ($G' < G''$). But as soon as the external strain was reduced to 1%, the G' value of the hydrogel quickly returned to a normal level, as shown in Figs. 3(d)–3(f), which serves as an excellent foundation for its possible use as an injectable medication or a cell delivery medium provided by its shear-thinning and recovery capabilities.

3.4 Biocompatibility studies

To exclude cell toxicity from the MSs, the CCK-8 assay was performed through the culturing of BMSCs with two types of MSs. Figure 4 shows the *in vitro* cytotoxicity evaluation results of two spheroids in different modes. BMSCs were cultured on both types of MSs in different modes for 1, 4, and 7 d, following which it was observed that the cells grew well on all types of MSs, and the number of cells increased with the prolonging of the culturing time. Cells growing on peptide-supported MSs are more than those on MSs, indicating that the peptide-supported MS-based culture modes (P-PLLA-MS and P-PS-MS) are conducive to the proliferation of cells, because they provide a larger SSA for cell attachment compared with that of pure MS culturing, facilitating the exchange of oxygen and nutrients.

3.5 Cell adhesion

Prior to the preparation of cell-loaded peptide-MS systems for cell expansion and regeneration, we investigated the adsorption of cells on microcarriers by exposing them to cell suspensions for the evaluation of cell adhesion ability of this type of biomimetic substitutes. It was reported that a wide range of cell types responded to topographic and chemical cues, thereby changing their cell morphology and function [38–39]. The detailed morphology of cells attached on the surface of MSs was observed by SEM (Fig. 5). After culturing for 1 d, most of the cells were attached on both types of MSs. Cells were attached on the frames and bridged pores of the surface of PLLA-MSs, some of which even extending into the pores (Fig. 5(b)). The enlarged images clearly showed that most of the cells had a well-spread and flattened morphology on MSs. It was known that cells only spread well when they are compatible with the surface of a material [40].

3.6 Characterization of cell-loaded peptide-MS systems

The effects of the culture conditions (static culture and peptide-supported culture) on the adhesion and growth of BMSCs on MSs were investigated *in vitro*. The peptide-supported culture was performed by the incubation of microcarriers in the peptide with a continuous supply of nutrients and oxygen, while the static culture was maintained in the fixed media volume. CLSM images in Fig. 6(a) depict that the calcein-labeled cells with green fluorescence gradually increased in number with the prolongation of the culturing time, while the dead cells labeled by PI (red fluorescence) were hardly observed, demonstrating that the cells distributed in such two MSs successfully proliferated. Compared with the static

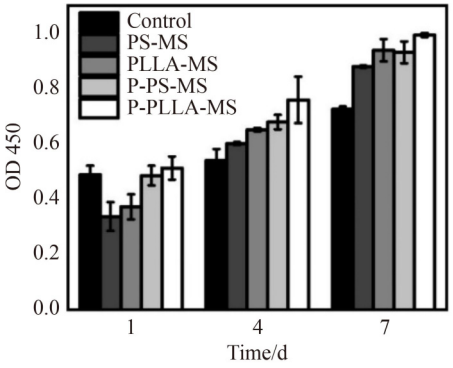

Fig. 4 *In vitro* cytotoxicity evaluation by the CCK-8 method.

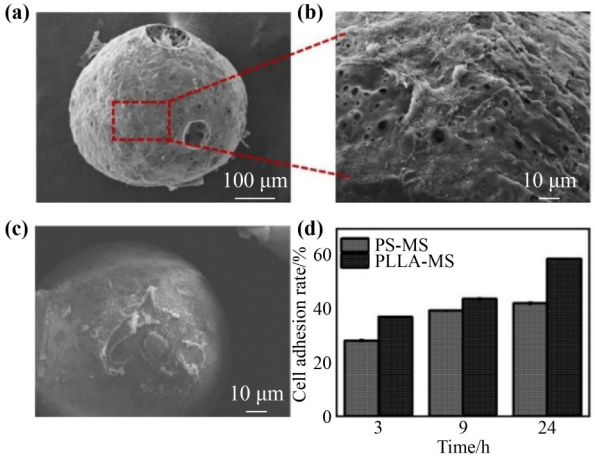

Fig. 5 SEM images of BMSCs on MSs cultured for 1 d: (**a**)(**b**) PLLA-MS; (**c**) PS-MS. (**d**) Adhesion of cells for different lengths of time (3, 9, and 24 h) under two MSs.

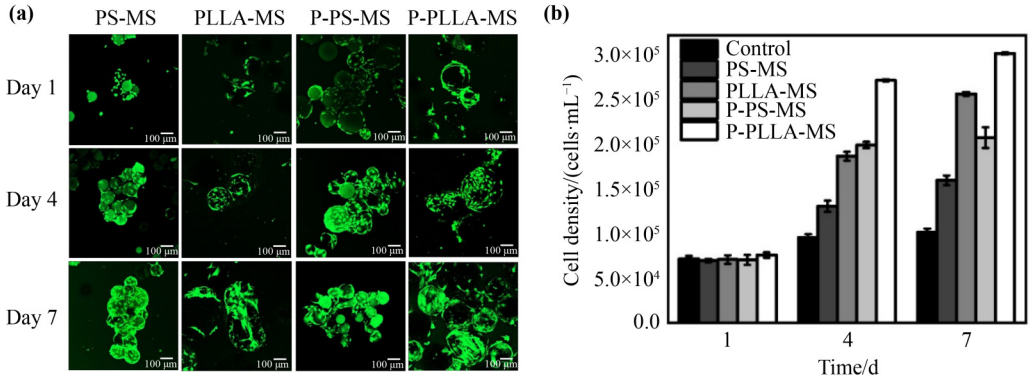

Fig. 6 (**a**) CLSM images of BMSCs in PS-MS, PLLA-MS, P-PS-MS, and P-PLLA-MS through the live/dead cell staining assay. (**b**) Cell densities of BMSCs in different culture modes.

culture, the cell distribution in the peptide-supported culture was more uniform with a higher cell density due to the continuous supply of nutrients and oxygen leading to faster proliferation [41–42]. In addition, it was observed that the adhesion rate of myoblasts was also higher in the peptide-supported culture compared to that of the static culture. Figure 6(b) depicts that the BMSCs had consistent growth and proliferation on microcarriers with monotonically increasing trends. The cell growth was slightly higher initially in the static culture method compared to that of the peptide-supported culture. However, the growth trend increased rapidly from the fourth day on in the peptide-supported culture and had shown a favorable growth. Together, the peptide-supported culture method was advantageous in cultivating cells at high density, which effectively promoted the growth of cells [43].

4 Conclusions

In summary, we successfully prepared two types of injectable porous MSs for *in vitro* expansion of stem cells. These biocompatible MSs have interconnected pathways that lead to a high degree of cell adhesion and rapid and sustained proliferation of stem cells. Cell experiments revealed that these MSs, supported by peptide scaffolds, have a strong promotional effect on cell proliferation. It is believed that in the cell culture system of peptide-supported MSs, stem cells and materials have more interaction with each other, which can ultimately promote efficient cell proliferation.

Declaration of competing interests The authors declare that they have no competing interests.

Acknowledgements This work was supported by the National Key Research and Development Program of China (Grant No. 2021YFC2101400).

References

[1] Zhang Y S, Khademhosseini A. Advances in engineering hydrogels. Science, 2017, 356(6337): eaaf3627

[2] Spicer C D. Hydrogel scaffolds for tissue engineering: the importance of polymer choice. Polymer Chemistry, 2020, 11(2): 184–219

[3] Sun W, Gregory D A, Zhao X. Designed peptide amphiphiles as scaffolds for tissue engineering. Advances in Colloid and Interface Science, 2023, 314: 102866

[4] Curvello R, Kast V, Ordóñez-Morán P, et al. Biomaterial-based platforms for tumour tissue engineering. Nature Reviews Materials, 2023, 8(5): 314–330

[5] El-Husseiny H M, Mady E A, El-Dakroury W A, et al. Smart/stimuli-responsive hydrogels: state-of-the-art platforms for bone tissue engineering. Applied Materials Today, 2022, 29: 101560

[6] Zhau H E, Goodwin T J, Chang S M, et al. Establishment of a three-dimensional human prostate organoid coculture under microgravity-simulated conditions: evaluation of androgen-induced growth and PSA expression. *In Vitro* Cellular & Developmental Biology: Animal, 1997, 33(5): 375–380

[7] Chen F, Le P, Fernandes-Cunha G M, et al. Bio-orthogonally crosslinked hyaluronate-collagen hydrogel for suture-free corneal defect repair. Biomaterials, 2020, 255: 120176

[8] Wang J, Chu R, Ni N, et al. The effect of Matrigel as scaffold material for neural stem cell transplantation for treating spinal cord injury. Scientific Reports, 2020, 10(1): 2576

[9] Jin K, Mao X, Xie L, et al. Transplantation of human neural

precursor cells in Matrigel scaffolding improves outcome from focal cerebral ischemia after delayed postischemic treatment in rats. Journal of Cerebral Blood Flow and Metabolism, 2010, 30(3): 534–544

[10] Koutsopoulos S, Zhang S. Long-term three-dimensional neural tissue cultures in functionalized self-assembling peptide hydrogels, matrigel and collagen I. Acta Biomaterialia, 2013, 9(2): 5162–5169

[11] Yang Z, Xu H, Zhao X. Designer self-assembling peptide hydrogels to engineer 3D cell microenvironments for cell constructs formation and precise oncology remodeling in ovarian cancer. Advanced Science, 2020, 7(9): 1903718

[12] Li X, Sun Q, Li Q, et al. Functional hydrogels with tunable structures and properties for tissue engineering applications. Frontiers in Chemistry, 2018, 6: 499

[13] Liu S Q, Tian Q, Hedrick J L, et al. Biomimetic hydrogels for chondrogenic differentiation of human mesenchymal stem cells to neocartilage. Biomaterials, 2010, 31(28): 7298–7307

[14] Liu S Q, Tian Q, Wang L, et al. Injectable biodegradable poly(ethylene glycol)/RGD peptide hybrid hydrogels for *in vitro* chondrogenesis of human mesenchymal stem cells. Macromolecular Rapid Communications, 2010, 31(13): 1148–1154

[15] Liu S Q, Ee P L R, Ke C Y, et al. Biodegradable poly(ethylene glycol)–peptide hydrogels with well-defined structure and properties for cell delivery. Biomaterials, 2009, 30(8): 1453–1461

[16] Motealleh A, Kehr N S. Nanocomposite hydrogels and their applications in tissue engineering. Advanced Healthcare Materials, 2017, 6(1): 1600938

[17] Elkhoury K, Russell C S, Sanchez-Gonzalez L, et al. Soft-nanoparticle functionalization of natural hydrogels for tissue engineering applications. Advanced Healthcare Materials, 2019, 8(18): 1900506

[18] Ahmed E M. Hydrogel: preparation, characterization, and applications: a review. Journal of Advanced Research, 2015, 6(2): 105–121

[19] Chen J, Zou X. Self-assemble peptide biomaterials and their biomedical applications. Bioactive Materials, 2019, 4: 120–131

[20] Koutsopoulos S. Self-assembling peptide nanofiber hydrogels in tissue engineering and regenerative medicine: progress, design guidelines, and applications. Journal of Biomedical Materials Research Part A, 2016, 104(4): 1002–1016

[21] Schop D, van Dijkhuizen-Radersma R, Borgart E, et al. Expansion of human mesenchymal stromal cells on microcarriers: growth and metabolism. Journal of Tissue Engineering and Regenerative Medicine, 2010, 4(2): 131–140

[22] Sart S, Errachid A, Schneider Y J, et al. Modulation of mesenchymal stem cell actin organization on conventional microcarriers for proliferation and differentiation in stirred bioreactors. Journal of Tissue Engineering and Regenerative Medicine, 2013, 7(7): 537–551

[23] He Q, Zhang J, Liao Y, et al. Current advances in microsphere based cell culture and tissue engineering. Biotechnology Advances, 2020, 39: 107459

[24] Zhang L, Zhang J, Ling Y, et al. Sustained release of melatonin from poly (lactic-co-glycolic acid) (PLGA) microspheres to induce osteogenesis of human mesenchymal stem cells *in vitro*. Journal of Pineal Research, 2013, 54(1): 24–32

[25] Wang C K, Ho M L, Wang G J, et al. Controlled-release of rhBMP-2 carriers in the regeneration of osteonecrotic bone. Biomaterials, 2009, 30(25): 4178–4186

[26] Tseng P C, Young T H, Wang T M, et al. Spontaneous osteogenesis of MSCs cultured on 3D microcarriers through alteration of cytoskeletal tension. Biomaterials, 2012, 33(2): 556–564

[27] Qu M, Xiao W, Tian J, et al. Fabrication of superparamagnetic nanofibrous poly(l-lactic acid)/γ-Fe_2O_3 microspheres for cell carriers. Journal of Biomedical Materials Research Part B: Applied Biomaterials, 2019, 107(3): 511–520

[28] Bai L, Han Q, Han Z, et al. Stem cells expansion vector via bioadhesive porous microspheres for accelerating articular cartilage regeneration. Advanced Healthcare Materials, 2024, 13(3): 2302327

[29] Lin A, Liu S, Xiao L, et al. Controllable preparation of bioactive open porous microspheres for tissue engineering. Journal of Materials Chemistry B: Materials for Biology and Medicine, 2022, 10(34): 6464–6471

[30] Maksoud F J, Velázquez de la Paz M F, Hann A J, et al. Porous biomaterials for tissue engineering: a review. Journal of Materials Chemistry B: Materials for Biology and Medicine, 2022, 10(40): 8111–8165

[31] Chen A K L, Reuveny S, Oh S K W. Application of human mesenchymal and pluripotent stem cell microcarrier cultures in cellular therapy: achievements and future direction. Biotechnology Advances, 2013, 31(7): 1032–1046

[32] Kim T K, Yoon J J, Lee D S, et al. Gas foamed open porous biodegradable polymeric microspheres. Biomaterials, 2006, 27(2): 152–159

[33] Shi X, Jiang J, Sun L, et al. Hydrolysis and biomineralization of porous PLA microspheres and their influence on cell growth. Colloids and Surfaces B: Biointerfaces, 2011, 85(1): 73–80

[34] Shi X, Sun L, Jiang J, et al. Biodegradable polymeric microcarriers with controllable porous structure for tissue engineering. Macromolecular Bioscience, 2009, 9(12): 1211–1218

[35] Shi X, Sun L, Gan Z. Formation mechanism of solvent-induced porous PLA microspheres. Acta Polymerica Sinica, 2011(8): 866–873 (in Chinese)

[36] Shi X, Cui L, Sun H, et al. Promoting cell growth on porous PLA microspheres through simple degradation methods. Polymer Degradation & Stability, 2019, 161: 319–325

[37] Chiu Y C, Cheng M H, Engel H, et al. The role of pore size on vascularization and tissue remodeling in PEG hydrogels. Biomaterials, 2011, 32(26): 6045–6051

[38] Huang C C, Wei H J, Yeh Y C, et al. Injectable PLGA porous beads cellularized by hAFSCs for cellular cardiomyoplasty. Biomaterials, 2012, 33(16): 4069–4077

[39] Andersson A S, Bäckhed F, von Euler A, et al. Nanoscale features influence epithelial cell morphology and cytokine production. Biomaterials, 2003, 24(20): 3427–3436

[40] Loesberg W A, te Riet J, van Delft F C, et al. The threshold at which substrate nanogroove dimensions may influence fibroblast alignment and adhesion. Biomaterials, 2007, 28(27): 3944–3951

[41] Rangarajan S, Madden L, Bursac N. Use of flow, electrical, and mechanical stimulation to promote engineering of striated muscles. Annals of Biomedical Engineering, 2014, 42(7): 1391–1405

[42] Berenzi A, Steimberg N, Boniotti J, et al. MRT letter: 3D culture of isolated cells: a fast and efficient method for optimizing their histochemical and immunocytochemical analyses. Microscopy Research and Technique, 2015, 78(4): 249–254

[43] Bueno E M, Bilgen B, Barabino G A. Wavy-walled bioreactor supports increased cell proliferation and matrix deposition in engineered cartilage constructs. Tissue Engineering, 2005, 11(11–12): 1699–1709